Purdue University

Purdue e-Pubs

International Refrigeration and Air Conditioning Conference

School of Mechanical Engineering

2012

Air-Side Heat Transfer Performance of Louver Fin and Multi-Tube Heat Exchanger for Fuel-Cell Cooling Application

Hiechan Kang
hckang@kunsan.ac.kr

Hyeonsik Oh

Minkyoo Lee

Anthony M. Jacobi

Jin Ho Kim

Follow this and additional works at: http://docs.lib.purdue.edu/iracc

Air-Side Heat Transfer Performance of Louver Fin and Multi-Tube Heat Exchanger for Fuel-Cell Cooling Application

Hie Chan KANG[1]*, Hyun Sik OH, Min Kyoo LEE, Hyejung CHO[2], Jin Ho KIM, Anthony M. JACOBI[3]

[1]Kunsan National University, School of Mechanical and Automotive Engineering
Gunsan, Jeonbuk, South Korea
(Phone 82-63-469-4722, Fax 82-63-469-4727, hckang@kunsan.ac.kr, ohs85@naver.com, lughmin86@naver.com)

[2]Samsung Electronics Co. Ltd., SAIT, Yongin, Gyeonggi, South Korea
(Phone 82-31-280-9433, Fax 82-31-280-9359, cho1115@samsung.com, jh527.kim@samsung.com)

[3]University of Illinois at Urbana-Champaign, Dept. of Mechanical and Science Engineering
Urbana, IL, USA
(Phone 1-217-333-4108, Fax 1-217-333-6534, a-jacobi@illinois.edu)

* Corresponding Author

ABSTRACT

The present work is performed to evaluate the heat transfer performance of a heat exchanger used in a fuel cell. Because of material constraints and performance requirements, a louver fin heat exchanger is modified for use with conventional micro-channel tubes and with multiple small-diameter tubes (a so-called multi-tube). Prototype heat exchangers are tested, and the air-side heat transfer, pressure drop, and fan power are measured in a wind tunnel and simulated using a commercial code. The air-side pressure drop and heat transfer coefficient of the multi-tubes show similar trends to those of the flat-tube heat exchanger if the contact resistance is negligible. The tube spacing of the prototype multi-tube heat exchangers has a small effect on the pressure drop and heat transfer, but it has a profound effect on air-side heat transfer performance because of the contact resistance between the tubes and louver fins. The air-side pressure drop agrees well with an empirical correlation for flat tubes.

1. INTRODUCTION

The direct methanol fuel cell (DMFC) is a proton-exchange fuel cell, in which methanol is used as the fuel. The advantage of DMFC is to use of methanol, a reasonably stable liquid at environmental conditions. DMFC has developed to portable or small mobile applications where energy and power density are more important than efficiency. Recently, DMFC is finding broader application, because of their low-noise operation, mobility, and nontoxic e. Fuel cells should be effectively cooled for efficiency, and normally exchangers are needed for the anode and cathode sides. However methanol is not compatible with most metals, so the choice of metal is very limited. The heat exchangers are operated by using a fan and motor, so effective cooling is very important in the total fuel cell system.

The louver fin and tube heat exchanger is one of the best candidates this application because of their performance, light weight, and low fan power. A large fraction of the total thermal resistance is on the air side of the louver fin heat exchanger. The configurations of the louver and tube greatly affect performance, cost, productivity, weight, etc. Much research has been conducted on the louver fin heat exchanger to improve heat transfer performance and reduce pressure drop. Kays and London (1984), Davenport (1983), Achaichia and Cowell (1988), Sunden and Svantesson (1992), Sahnoun and Webb (1992), Park and Jacobi (2009) and Kang and Jun (2011) presented empirical data and suggested correlations for louver fins. Gupta (2010) reported on the air side drainage and heat transfer performance of louver fin heat exchangers with drainage channels in their flat tubes.

The present study considers a multi-tube and louver fin heat exchanger modified from the conventional flat tube or micro channel tube base heat exchanger. Experiments and numerical simulations were conducted for heat exchangers having six kinds of multi-tubes and flat tubes to investigate their performance.

2. EXPERIMENTAL AND NUMERICAL METHODS

2.1 Tested Heat Exchangers
The tube shapes of louver fined heat exchangers are classified as flat tube and the micro-channel tube as shown in Figure 1 (a) and (b). The present work considers a multi-tube louver fin heat exchanger as shown in Figure (c)—the equally spaced circular tubes replace the flat tube. The merit of the geometry is that it gives more choices of tube material and substitutive machining process instead of flat or micro channel. The performance of tube inside and outside of multi-tube heat exchanger can be maintained as similar with the conventional louver fin tube heat exchanger. Table 1 shows the multi-tube and flat tube geometries of the present work. The tubes are placed with equal spacing along the air flow direction (x).The test parameters are the shape of tube (flat tube and multi-tube), fin depth (F_d) (24.6 mm and 32.0 mm), and multi-tube pitch (p_l) (2.48 mm (NT13), 3.30 mm (NT10), and 4.95 mm (NT7)). The tube width of the flat tube was the same as the tube diameter of multi-tube to maintain the tube and louver layout. The louver fin configuration such as fin pitch, louver pitch, louver angle and fin thickness were the same in all cases. The tube and fin were made of stainless steel and copper, respectively, and the face area was 0.25 m by 0.25 m. Two prototype heat exchangers MT32NT10 and MT24NT11 were constructed for experiments and four cases (FT32, MT32NT13, MT32NT10, MT32NT7) were simulated numerically.

Table 1: Dimensions of Louver Fin Heat Exchangers Tested in the Present Work (Unit in mm and degree)

Tube Shape	-	Flat Tube		Multi-Tube			
HEX ID	Symbol	FT24	FT32	MT24NT11	MT32NT13	MT32NT10	MT32NT7
Fin Depth	F_d	24.6	32.0	24.6	32.0	32.0	32.0
Fin Pitch	F_p	1.43	1.43	1.43	1.43	1.43	1.43
Fin Height	H	7.50	7.50	7.50	7.50	7.50	7.50
Louver Pitch	L_p	1.30	1.30	1.30	1.30	1.30	1.30
Louver Angle	θ	30	30	30	30	30	30
Fin Thickness	F_{th}	0.05	0.05	0.05	0.05	0.05	0.05
Tube Pitch	T_p	9.1	10.0	9.1	10.0	10.0	10.0
Tube Depth	T_d	24.6	32.2	24.6	32.2	32.2	32.2
Number of Tube	N_t	1	1	11	13	10	7
Longitudinal Tube Pitch	P_l	-	-	2.30	2.48	3.30	4.95
Tube Outside Diameter	D_o	-	-	1.60	2.5	2.5	2.5
Performance Evaluation Method		Correlation	Correlation CFD	Experiment CFD	CFD	Experiment CFD	CFD
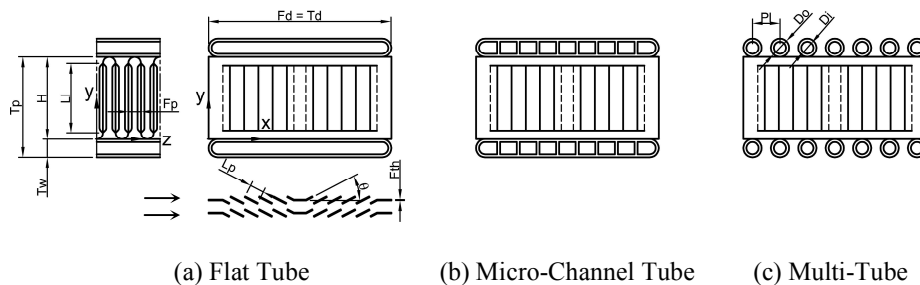
(a) Flat Tube   (b) Micro-Channel Tube   (c) Multi-Tube
Figure 1: Brazed Louver Fin Heat Exchangers Having Different Tube Patterns

2.2 Numerical Method

The air-side pressure drop and heat transfer performance of louver fins were simulated by the commercial CFD code CFX 13 (ANSYS) in the present work. Test geometries in the numerical simulation are as shown in Table 1 and Figure 1. The calculation domain was two fins and free airflow regions of 10 and 30 times the hydraulic diameters at the airflow inlet and outlet to simulate practical conditions. The air flow was assumed to be three dimensional, laminar, and steady-state, without natural convection and conjugate heat conduction in the fin. The properties of air and fin were assumed to be constant for air and copper at atmospheric pressure. A tetrahedral mesh (981,000-1,641,000) was used after a mesh quality dependency test, and the surface mesh of the flat tube (FT32) and multi-tube and louver fin (MT32NT10) shown in Figure 2. It is assumed that the fin and multi-tube are completely brazed, and 1/4 of tube diameter of multi-tube are blocked by the brazing flux at the narrow gap of inter tube region. The inlet air velocities were uniform at 1.0, 2.0 and 4.0 m/s, and the temperatures of the inlet air and fin bases were constant at 20°C and 80°C respectively. The inlet and exit boundary conditions were applied at the inlet and exit, the wall boundary conditions at the fin surface and flat tube, and periodic boundary conditions were applied at the two mid planes of the fins. The convergence criteria were 3x10^{-4} for the residual sum of the mass and 0.07% for the energy balance.

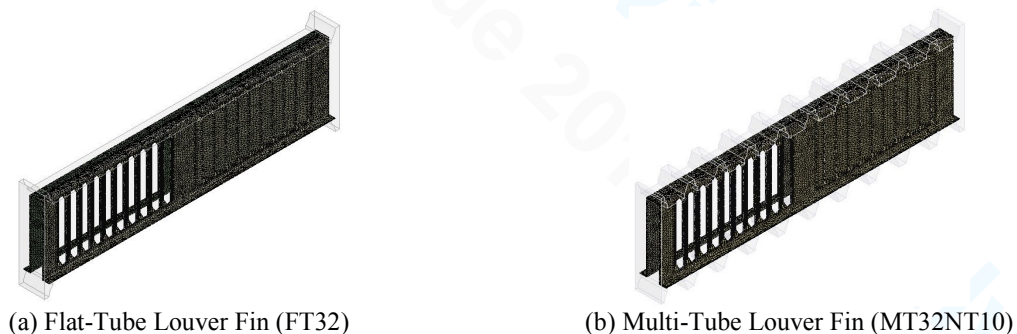(a) Flat-Tube Louver Fin (FT32)   (b) Multi-Tube Louver Fin (MT32NT10)

Figure 2: Numerical Surface Grids in the Present Work

2.2 Experimental Method

The air-side performance of two prototype heat exchangers was measured using a wind tunnel and water bath. The wind tunnel was a suction and open loop type. It consisted of a fan for air flow, an inlet heat exchanger to acquire uniform and constant inlet temperature, a main test section and an exit chamber for measuring the air flow rate. The frontal air velocity ranged from 1.3 to 4.2 m/s by controlling fan speed. The dimensions of the main test section were 250 mm in width, 250 mm in height, 400 mm in length. Side walls of the heat exchanger were insulated with 20 mm of rubber form (k=0.041 W/m K) to minimize heat loss. In the exit chamber, a 150.0 mm diameter flow nozzle was installed to measure the air flow rate. Four screens were installed to provide a flat velocity profile upstream and downstream of the flow nozzle. The water bath fed constant temperature water to the prototype heat exchangers. The water flow rate was 2.2 l/min and controlled by the constant flow rate pump. The air inlet state was 22±1°C at atmospheric pressure, and the water inlet was 49±1°C. The flow rate and air side pressure drop were measured by pressure transducers (±0.5 Pa). The inlet and exit temperatures of the air were measured by the 13 K-type thermocouples (±0.1°C). The inlet and exit temperatures of water were measured using three wire RTDs (±0.05°C). Each experiment was operated more than 2 hours to get steady state conditions, and the energy balance between water and air sides was within 7.5%.

In a standard wind tunnel test, the total thermal resistance is made up of three resistances of water-side (tube-side), tube wall and air-side (fin-side) as follows

$$\frac{1}{UA} = \frac{1}{h_t A_t} + R_w + \frac{1}{\eta_s h A_o} \tag{1}$$

In the above, *UA* is the overall heat conductance, and *h* is the heat transfer coefficient. The surface efficiency η_f is expressed as

$$\eta_s = \left(A_{tube} + \eta_{fin} A_{fin}\right)/A_o \tag{2}$$

$$\eta_{fin} = \frac{\tanh(mH/2)}{mH/2} \tag{3}$$

$$m = \sqrt{\frac{2h}{k_{fin}F_{th}}} \tag{4}$$

The A_{fin}, A_{tube}, and A_o denote the fin, tube and total surface areas for the air-side. The measured pressure drop, ΔP_{mea}, includes the entrance, acceleration and exit losses as follows, and the frictional pressure drop is found by accounting for these effects:

$$\Delta P = \Delta P_{mea} - \frac{\rho_{in}u_{c,in}^2}{2}\left(1 - \sigma^2 + K_c\right) - \left(\rho_{ex}u_{c,ex}^2 - \rho_{in}u_{c,in}^2\right) - \frac{\rho_{ex}u_{c,ex}^2}{2}\left(1 - \sigma^2 - K_e\right) \tag{5}$$

The K_c and K_e in the above equation were obtained from Kays and London (1984), and σ is the contraction ratio which is the ratio of the minimum cross section to the frontal area. The friction factor f, the modified Colburn j-factor and the Reynolds number are defined as

$$f = \frac{2\,A_c\,\Delta P}{\rho A_o\,u_c^2} \tag{6}$$

$$j = \frac{\eta_s h\,\mathrm{Pr}^{2/3}}{\rho u_c c_p} \tag{7}$$

$$\mathrm{Re}_{Lp} = \frac{\rho u_c L_p}{\mu} \tag{8}$$

where u_c is maximum velocity in the minimum free-flow area. The water side heat transfer coefficient is estimated by the following equations.

$$\mathrm{Nu}_t = 3.66, \text{ for } \mathrm{Re}_t < 2300 \tag{9}$$

$$\mathrm{Nu}_t = \frac{(f_t/8)(\mathrm{Re}_t - 1000)\mathrm{Pr}_t}{1 + 12.7(f_t/8)^{1/2}\left(\mathrm{Pr}_t^{2/3} - 1\right)}, \text{ for } \mathrm{Re}_t > 2300 \tag{10}$$

$$\mathrm{Nu}_t = \frac{h_t D_i}{k_t} \tag{11}$$

The friction coefficient of water-side f_t was obtained by Moody chart. Measurement errors at a frontal air velocity of 1.7 m/s were: differential pressure of the nozzle flow meter was evaluated as ±2.0%, pressure drop ±0.5 Pa, and air temperatures ±0.1°C. Through standard propagation of error analysis, the error for Re_{Lp} and f and j factors were calculated as 1.8%, 2.3%, and 3.6%, respectively, at a 95% confidence level.

3. RESULTS AND DISCUSSION

### 3.1 Flow and Heat Transfer Characteristics
Figure 3 shows the streak lines of the air flow for the flat tube and louver fin (FT32) and the multi-tube (MT32NT7) at a frontal velocity of 2 m/s. The air velocity was high across the louvers and low near the flat and multi-tubes. The main stream showed V-shaped patterns in the *x-y* plane and weak zigzag lines in the *x-z* plane. The air velocity was concentrated at the centers of the louvers at the inlet, and distributed width wise along the airflow direction. Vortices were observed in the inter-tube region of the multi-tube heat exchanger. In the multi-tube heat exchanger, the

velocity across the louvers was higher than for the flat-tube case, because the vortices pushed the main airflow into the louver area.
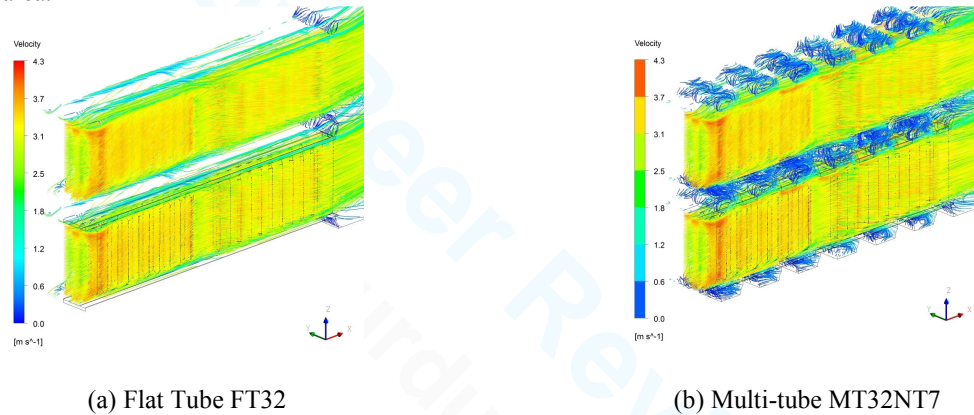
(a) Flat Tube FT32   (b) Multi-tube MT32NT7
Figure 3: Streak lines of Test Heat Exchangers at Frontal Velocity of 2 m/s

Figure 4 shows the isotherm contours of air in the middle plane and at the fin surfaces with the frontal air velocity of 2 m/s, for the flat tube (F32) and multi-tube (MT32NT10) heat exchangers. The air temperature was monotonically increased while passing through each louver because of the high heat transfer coefficient. The fin temperature changed about 10 K, being lowest at the center of the first louver. Cold spots were observed near the inter-tube region of the multi-tube heat exchanger. However, they changed the fin efficiency little.
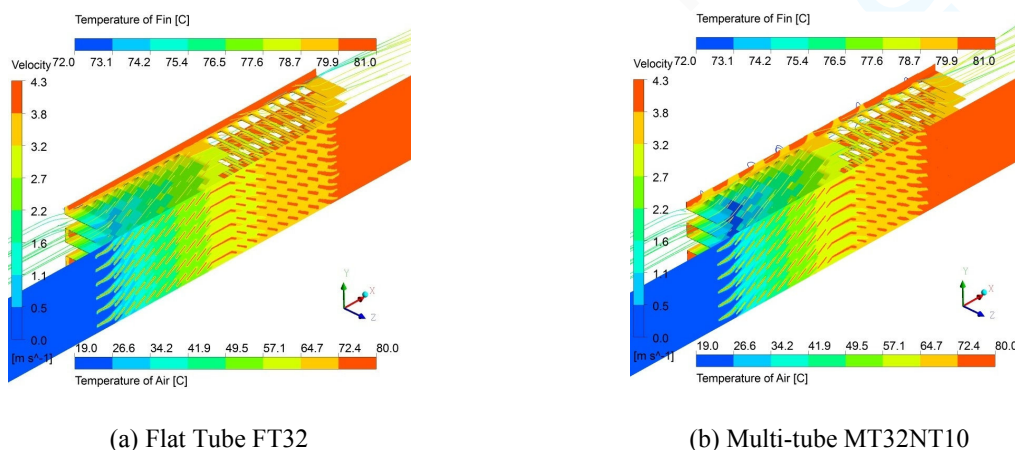
(a) Flat Tube FT32   (b) Multi-tube MT32NT10
Figure 4: Isotherm Contours of Air in Middle Plane and at Fin Surfaces with Frontal Velocity of 2 m/s

Figure 5 shows the shear stress distribution on the fin and tube surfaces at the frontal air velocity of 2 m/s for the flat tube (F32) and multi-tube (MT32NT10) heat exchangers. The shear stress for each louver was almost the same, and that for the middle louver was relatively small. The shear stress on the non-louvered surface was smaller than that on the louver surface. The shear stress on the louvers of the multi-tube was a little higher than on those of the flat-tube because of the higher air velocity; however, it was near zero on the multi-tube surfaces.
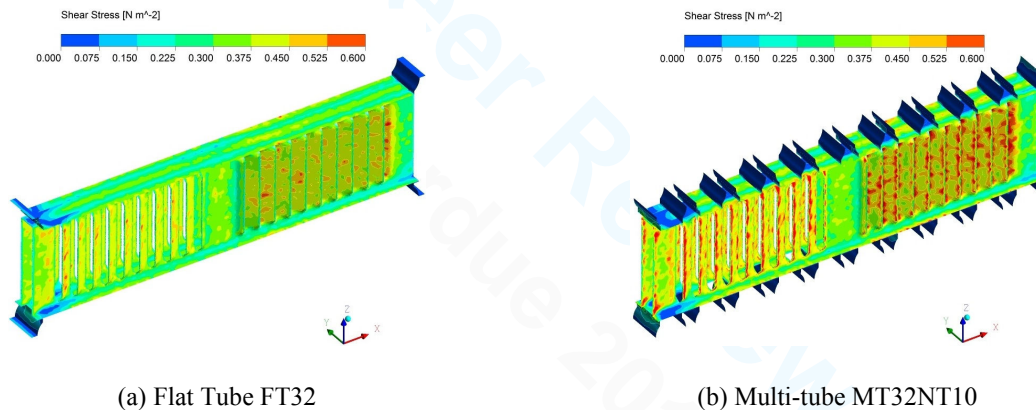
Figure 6 shows the heat flux distribution on the fin and tube surfaces for the same cases as Figure 5. The heat flux was highest at the inlet, decreased along the flow direction, and was relatively high in the center plane of the louvers, because of the temperature difference between the fin surfaces and the air. Comparing the two heat exchangers, the multi-tube one showed a higher heat flux at the airflow inlet, but a smaller one at the exit.

### 3.2 Air-Side Pressure Drop and Heat Transfer
Figures 7, 8, and 9 show comparisons of the air-side pressure drop, heat transfer coefficient, and f and j factors of the present heat exchangers. The measured pressure drops of the prototype multi-tube heat exchangers MT32NT10 and MT24NT11 were 7% and 12% lower, respectively, than predictions from the correlation of Kang and Jun

(2011). The measured and calculated f factors of the multi-tube and flat-tube were similar experimentally and numerically, agreeing well with the correlations, as shown in Figure 9. The tube distance of the multi-tube affected its pressure drop very little. The reason is that the air-side pressure drop depends on the louver fin much more than on the tube. In the numerical results, the multi-tube MT32NT10 showed an 18% higher pressure drop than the flat tube FT32.

(a) Flat Tube FT32   (b) Multi-tube MT32NT10
Figure 5: Shear Stress Distribution on Fin and Tube Surfaces at Frontal Velocity of 2 m/s
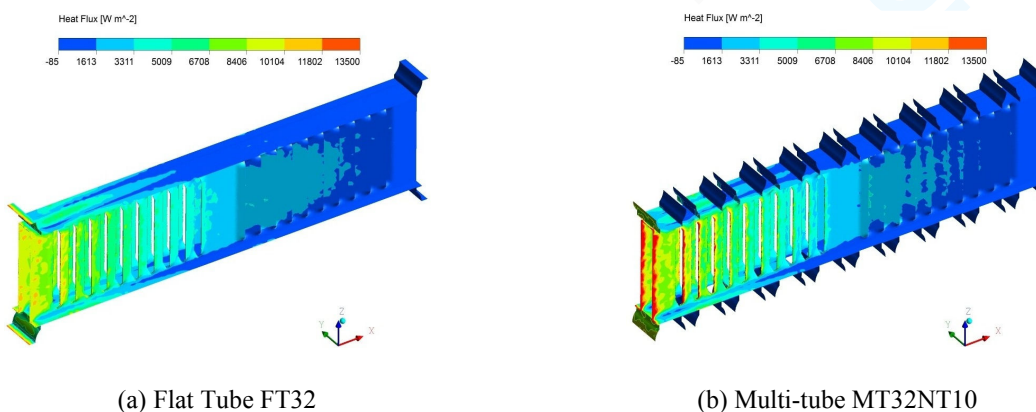
(a) Flat Tube FT32   (b) Multi-tube MT32NT10
Figure 6: Heat Flux Distribution on Fin and Tube Surfaces at Frontal Velocity of 2 m/s

The measured heat transfer coefficient of the prototype multi-tube heat exchangers MT32NT10 and MT24NT11 were 63% and 71% lower than the predictions of Kang and Jun, as shown in Figure 8. The reason may be because of contact resistance between the louver fin and multi-tube: the multi-tube connects with the louver fin has shorter contact line, while the flat tube has a better line of contact. The numerical results of the air-side heat transfer coefficients of the flat-tube and multi-tube agreed with the correlations of Kang and Jun. In the present numerical simulation, the fins were assumed to be well-brazed to the multi-tubes. The heat transfer coefficient of the multi-tube was about 3% higher than that of the flat-tube. The effect of tube distance on the air-side heat transfer was small in the present multi-tube heat exchangers. Therefore, the conductance between the fin and multi-tube and the louver pattern are very important in the heat transfer performance of the multi-tube heat exchanger.

3.3 Fan Power Consumption
Figure 10 shows a comparison of the air-side specific heat transfer of the tested heat exchangers versus the specific fan power. The specific heat transfer is defined as the heat transfer rate per air-side temperature difference and heat exchanger volume ($A_o h / A_{fr} F_d$); the specific fan power on the horizontal axis is the fan power per heat exchanger volume ($W_{fan} / A_{fr} F_d = u_{fr} \Delta P / F_d$). The net fan power means the product of the air-side pressure loss and volume

flow rate, and the actual fan power was estimated by the electric power consumption of the fan motor. The net and actual fan powers are expressed by the solid and crossed circles and squares in Figure 10. The actual heat transfer performance of the prototype heat exchangers was about 30% to 34% of the ideal air-side performance estimated by the empirical correlations for flat-tube heat exchangers having the same louver fin layout at $u_{fr}\Delta P/F_d = 10^4$ W/m^3.

It is supposed that the main reason for the performance loss was the contact resistance between fins and tubes as discussed in section 3.2. Comparing the numerical results (hollow symbols), a multi-tube heat exchanger showed a 10 to 15% better heat transfer coefficient than did a flat-tube one for the same fan power. In the comparison of the net and real performances of the MT32NT10 and MT24NT11, the motor and fan shroud resulted in about a 5% loss in transferred heat for the same fan power. At the same thermal duty of $A_o h/A_{fr}F_d = 8\times10^4$ W/m^{3}K, the small fin-depth heat exchanger MT24NT11 needed about 30% of the fan power of the large fin-depth MT32NT10. Therefore, the heat exchanger design layout and quality manufacturing processes including brazing are important in the louver fin-type heat exchanger for the DMFC.
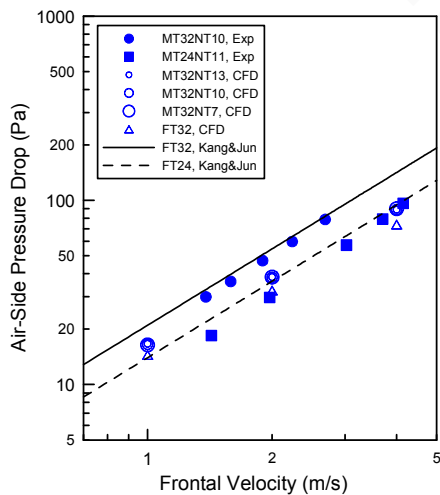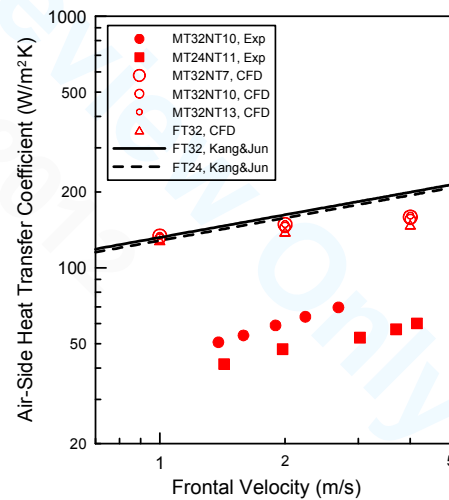

Figure 7: Comparison of Air-side Pressure Drop

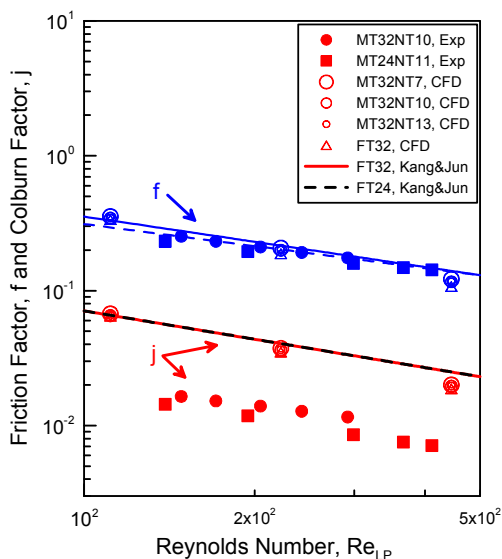**Figure 8:** Comparison of Air-side Heat Transfer Coefficient

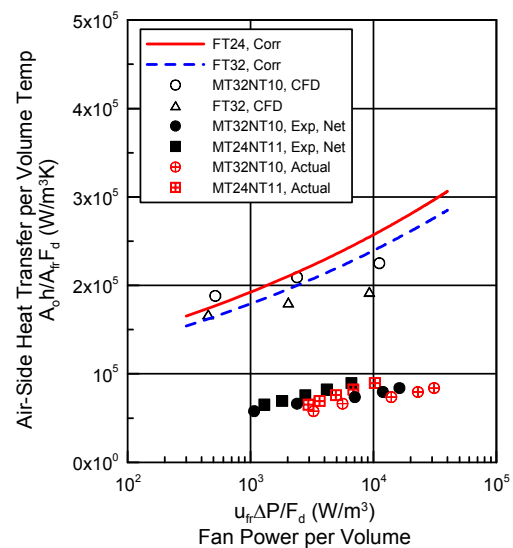**Figure 9:** Comparison of Air-Side f and j Factors

Figure 10: Comparison of Heat Transfer Performance versus Air-Side Fan Power for Same Heat Exchanger Volume and Flow Depth

5. CONCLUSIONS

In this study experiments and numerical simulations were performed on louver fin, multi-tube heat exchangers modified from the conventional louver fin, flat-tube heat exchanger. Six tube geometries with the same louver fin layout were investigated for the effects of the tube patterns on the air-side thermal and hydraulic performance. The following conclusions are drawn from the results:

- The air-side pressure drop and heat transfer coefficient of the multi-tube models showed generally similar trends to those of the flat-tube standard if the contact resistance was negligible. The tube space of the multi-tube heat exchanger had little effect on the pressure drop or heat transfer.
- The prototype multi-tube heat exchanger showed a large reduction of air-side heat transfer rate compared to the predicted heat transfer rate, because of the contact resistance between the tubes and fins. However, the air-side pressure drops of the multi-tube heat exchangers agreed reasonably well with the empirical correlations for the flat-tube exchangers.
- The louver fin, multi-tube heat exchanger delivered about a 10 to 15% higher heat transfer performance than the flat-tube for the same fan power and heat exchanger volume. For the same heat exchanger volume, a smaller fin depth is recommended to reduce the necessary fan power. Reduction of the contact resistance between the louver fins and multi-tubes is one of the important parameters to enhance the heat transfer performance.

NOMENCLATURE

A_o	air-side surface area of heat exchanger	(m^2)	**Greek Symbols**			
A_c	minimum flow area of heat exchanger	(m^2)	η_s	surface efficiency	(-)	
A_{fin}	fin surface area of heat exchanger	(m^2)	η_{fin}	fin efficiency	(-)	
A_{fr}	frontal area of heat exchanger	(m^2)	θ	louver angle	(deg)	
A_t	tube surface area of heat exchanger	(m^2)	σ	contraction ratio	(-)	
c_p	specific heat capacity	(J/kgK)				
D_i	tube inside diameter	(m)				
D_o	tube outside diameter	(m)				
f	pressure drop coefficient of air-side	(-)				
f_t	friction coefficient of tube-side	(-)				
F_d	depth of fin along the flow direction	(m)				
F_p	fin pitch	(m)				
F_{th}	fin thickness	(m)				
H	fin height	(m)				
h	air-side heat transfer coefficient	(W/m^2K)				
h_t	water-side heat transfer coefficient	(W/m^2K)				
j	air-side Colburn j factor	(-)				
k_{fin}	thermal conductivity of fin	(W/mK)				
k_t	thermal conductivity of water	(W/mK)				
L_p	louver pitch	(m)				
N_t	Number of tube	(-)				
Nu_t	Nusselt number of tube-side	(-)				
Pr	Prandtl number of air	(-)				
Pr_t	Prandtl number of water	(-)				

ΔP	air-side pressure drop	(Pa)
Re_{Lp}	Reynolds number based on louver pitch	(-)
Re_{t}	Reynolds number of tube-side	(-)
T_{p}	tube pitch	(-)
T_{d}	tube depth	(-)
ΔT_{ln}	logarithmic mean temperature difference	(K)
u_{fr}	frontal velocity	(m/s)
u_{c}	maximum velocity on minimum section	(m/s)
W_{fan}	fan power	(W)

REFERENCES

Achaichia, A., and Cowell, T. A., 1988, Heat Transfer and Pressure Drop Characteristics of Flat Tube and Louvered Plate Fin Surfaces, *Experimental Thermal and Fluid Science*, No. 1, pp. 147-157.

British Standard Institution, 1964, *Method for the Measurement of Fluid Flow in Pipes: Part 1: Orifice Plates, Nozzles and Venturi Tubes*, British Standard 1042, London.

ANSYS CFX, *Training Manual Release 13*, 2011, ANSYS, Inc.

Davenport, C. J., 1983, *Correlation for Heat Transfer and Flow Friction Characteristics of Louvered Fin*, AIChE Symp. Ser., 79, pp. 19-27.

Gupta, D, 2010. Air-side condensate management: drainage channels in heat exchangers, MS Thesis, University of Illinois at Urbana-Champaign.

Kang, H. C. and Jun, G. W, 2011, Heat Transfer and Flow Resistance Characteristics of Louver Fin Geometry for Automobile Applications, *ASME J. of Heat Transfer*, Vol. 133, 101802-1.

Kang, H. C., and Webb, R. L., 1998, Performance Comparison Enhanced Fin Geometries Used in the Fin-and-Tube Heat Exchangers, *Proceedings of the 11th Int. Heat Transfer Conference*, 6, pp. 273-278.

Kanjino, M., and Hiramatsu, M., 1987, *Research and Development of Automotive Heat Exchangers, in Heat Transfer in High Technology and Power Engineering*, Yang, W. J. and Mori, Y. ed., Hemisphere, Washington, D. C., pp. 420-432.

Kays, W. M., and London, A. L., 1984, *Compact Heat Exchangers, 3rd ed.*, McGraw-Hill, New York.

Park, Y. G. and Jacobi, A. M., 2009, The Air-Side Thermal-Hydraulic Performance of Flat-Tube Heat Exchangers With Louvered, Wavy, and Plain Fins Under Dry and Wet Conditions, *ASME J. of Heat Transfer*, Vol. 131, 061801-1

Sahnoun, A., and Webb, R. L., 1992, Prediction of Heat Transfer and Friction for Louver Fin Geometry, *ASME J. of Heat Transfer*, 114, pp. 893-899.

Sunden, B., and Svantesson, J., 1992, Correlation of j and f Factors for Multi-Louvered Heat Exchanger Surfaces, *Proceedings of the 3rd UK National Heat Transfer Conf.*, pp. 805-811.

Webb, R. L., 1994, *Principles of Enhanced Heat Transfer*, John Wiley & Sons, New York.

ACKNOWLEDGEMENT